ELSEVIER

Journal of Organometallic Chemistry 504 (1995) 93–105

Journal of Organometallic Chemistry

Ab initio molecular orbital study of oxidative addition of H_2 and CH_4 to the $RhCl(CO)(PH_3)_2$ complex

Djamaladdin G. Musaev, Keiji Morokuma *

Cherry L. Emerson Center for Scientific Computation and Department of Chemistry, Emory University, Atlanta, GA 30322, USA

Received 30 January 1995; in revised form 6 April 1995

Abstract

The restricted Hartree–Fock (RHF) and second order Møller–Plesset perturbation (MP2) methods were used to study the structure and stability of the complex $RhCl(CO)(PH_3)_2$, as well as its reactivity to molecules H_2 and CH_4. *trans*-$RhCl(CO)(PH_3)_2$ is about 13 kcal mol^{-1} more stable than *cis*-$RhCl(CO)(PH_3)_2$. The isocarbonyl *trans*-$RhCl(OC)(PH_3)_2$ isomer, where the CO ligand is coordinated to the metal atom by the oxygen atom, lies about 60 kcal mol^{-1} higher than carbonyl *trans*-$RhCl(CO)(PH_3)_2$ and is separated from the latter with a small isomerization barrier of 6 kcal mol^{-1}. The oxidative addition reactions *trans*-$RhCl(CO)(PH_3)_2 + H_2 \rightarrow (H)_2RhCl(CO)(PH_3)_2$ and *trans*-$RhCl(CO)(PH_3)_2 + CH_4 \rightarrow H(CH_3)RhCl(CO)(PH_3)_2$ take place without forming pre-reaction van der Waals complexes, and are calculated to be exothermic by 2 kcal mol^{-1} and endothermic by 20 kcal mol^{-1} and to have barriers of 16 and 27 kcal mol^{-1}, respectively. The reactions of less populated *cis*-$RhCl(CO)(PH_3)_2$ have comparable barriers, 18 and 31 kcal mol^{-1}, for H_2 and CH_4, respectively, and will not make major contributions to the mechanism of reaction of $RhCl(CO)(PH_3)_2$. These reactions of $RhCl(CO)(PH_3)_2$ should be substantially more difficult than the corresponding reactions of $RhCl(PH_3)_2$. The CO binding energies in the product $OC–[H(R)RhCl(PH_3)_2]$ are calculated to be 17 and 20 kcal mol^{-1} for R = H and CH_3, respectively, and the CO molecule will dissociate from the product at moderate temperatures.

Keywords: Rhodium; Oxidative addition; Ab initio calculations

1. Introduction

Although the Wilkinson catalyst, $RhCl(PPh_3)_3$, is one of the most widely used catalysts for activation of H–H, C–H and C–C bonds [1–4], the complex $RhCl(CO)(PPh_3)_2$ formed readily from $RhCl(PPh_3)_3$ by CO addition or aldehyde decarbonylation [4] shows limited reactivity with hydrocarbons and hydrogen [5], in contrast with its Ir(I) analog, the Vaska complex, which has been the subject of several experimental and theoretical studies [6]. Recently, Duckett and Eisenberg have also reported the oxidative addition of the H_2 molecule to the $RhCl(CO)(PPh_3)_2$ complex using the *para*-hydrogen-induced polarization method [7]. The H_2 oxidative addition to this d^8 Rh(I) complex yields an octahedral d^6 six-coordinate adduct that is very labile to CO loss and readily forms binuclear species [7]:

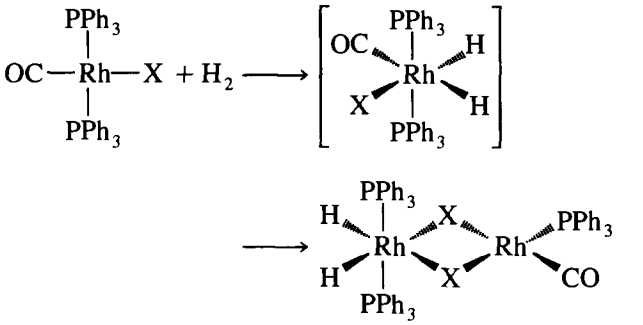

(1)

However, both the mechanism of the oxidative addition reaction of H_2 and alkanes to $RhCl(CO)(PPh_3)_2$, and the structure and stability of the reactant $RhCl(CO)(PPh_3)_2$, the expected transition state and intermediates need to be studied. Here the quantum

* Corresponding author.

Elsevier Science S.A.
SSDI 0022-328X(95)05612-2

chemical studies may be very useful. Early theoretical studies [8] on oxidative addition of the H_2 to the d^8 planar-square complex $RhCl(CO)(PH_3)_2$ using extended Hückel or limited ab initio methods led to the same conclusions, at least qualitatively; H_2 approaches the transition metal in the end-on mode in the early stage (up to an interaction distance of 2 Å) of the reaction and then rotates to give a side-on complex [8a,b,c]. The addition in the P–Rh–CO plane was favored as a result of a stabilizing backbonding interaction between the metal and CO ligand in the five-coordinate transition state [8d].

In the present paper we study the mechanism of the following model reactions:

$$RhCl(CO)(PH_3)_2 + H_2 \rightarrow (H)_2RhCl(CO)(PH_3)_2 \quad (2)$$

$$RhCl(CO)(PH_3)_2 + CH_4 \rightarrow H(CH_3)RhCl(CO)(PH_3)_2 \quad (3)$$

with an ab initio molecular orbital (MO) method, with three main goals: (i) to determine the geometrical structures and energies of the reactants, intermediates, transition states and the products of the reactions (2) and (3);

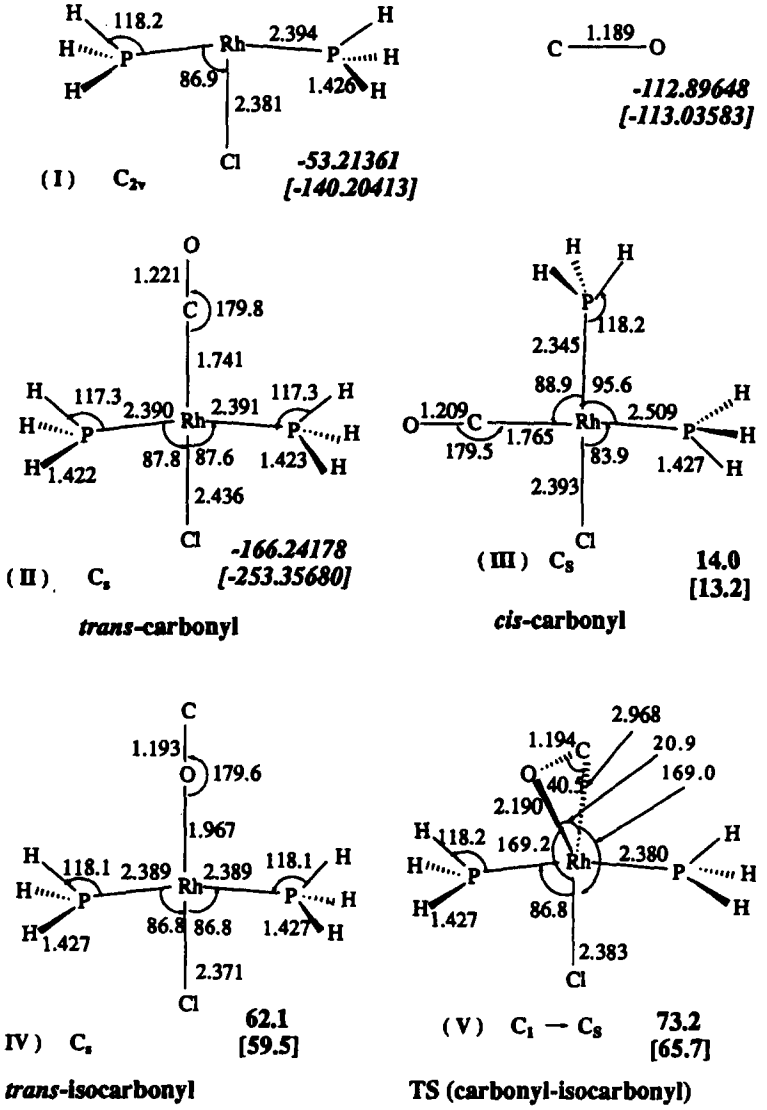

Fig. 1. Geometries and energies (total energies in hartrees in italics for reference structures, and relative energies in kcal mol^{-1} for others) of the alternative structures of the $RhCl(CO)(PH_3)_2$ complex, as well as the molecules $RhCl(PH_3)_2$ and CO, calculated at the MP2/I//MP2/I and MP2/II//MP2/I (in brackets) levels of theory. Assumed symmetry constraints are also shown; the notation $C_1 \rightarrow C_s$ means optimization under C_1 symmetry converged to a C_s structure.

(ii) to elucidate the differences and similarities between the H–H and C–H bond activation processes (2) and (3) on the saturated 16e $RhCl(CO)(PH_3)_2$ complex, and (iii) to examine the role of the additional CO ligand on the H–H and C–H bond activation by comparison of the reactions (2) and (3) with the corresponding reactions (4) and (5) of the unsaturated 14e $RhCl(PH_3)_2$ studied theoretically in detail by Koga and Morokuma [9,10].

$$RhCl(PH_3)_2 + H_2 \rightarrow (H)_2RhCl(PH_3)_2 \quad (4)$$

$$RhCl(PH_3)_2 + CH_4 \rightarrow H(CH_3)RhCl(PH_3)_2 \quad (5)$$

In the past ten years we have carried out ab initio theoretical studies of various CH activations and related problems. Some of important papers and a review article by us on the topic are given in Refs. [11–15].

2. Computational methods

We used two basis sets denoted I and II, respectively. The smaller basis set I, used mostly for geometry optimization of the critical structures, consists of the basis functions (9s5p/3s2p) [16] for C and O, (4s/2s) [16] for H, (3s3p4d/2s2p2d) [17] for Rh, (3s3p1d/2s2p1d) [18] ($\alpha_d = 0.39$ [19] and 0.50 [19] for P and Cl, respectively) for P and Cl, in conjunction with the Hay–Wadt relativistic effective core potentials [17,18], explicitly considering only 5s4d, i.e. nine valence electrons for Rh and 3s3p electrons, and five and seven electrons for P and Cl, respectively. The larger basis set II, used to calculate the energy at the critical points of the potential energy surface of the reactions (2) and (3), consists of the basis functions (9s5p1d/4s2p1d) [16] ($\alpha_d = 0.75$ [19] and 0.80 [19] for atoms C and O, respectively) for C and O, (4s1p/2s1p) [16] ($\alpha_p = 1.0$ [19]) for H, (5s5p4d/3s3p3d) for Rh, in conjunction with the relativistic effective core potential explicitly considering 17 electrons in 4s4p4d5s shells for Rh [20], with those for P and Cl in basis set I.

The geometry optimization was carried out with the basis set I by the restricted Hartree–Fock (RHF) and the second order Møller–Plesset perturbation (MP2) energy gradient methods. In calculations of local minimum structures, the $Rh–P^1H_3$, $Rh–P^2H_3$ and $Rh–CH_3$ fragments were assumed to have local C_{3v}-symmetry and were optimized just for one $P^1–H$, $P^2–H$ and C–H distance and one RhP^1H, RhP^2H and RhCH angle, respectively. The C_{2v} and C_s symmetry constraints were used for $RhCl(PH_3)_2$ (structure I) and $(CO)RhCl(PH_3)_2$ (structures II–IV), respectively. The transition state connecting carbonyl and isocarbonyl isomers of the $(CO)RhCl(PH_3)_2$ (structure V) was optimized without symmetry constraint. For reactions (2) and (3), the products VI, VII, X, XVIII, XIX and XXV and transition states XIII and XIV were calculated under C_s symmetry constraint, and the remaining products, transition states and anticipated intermediates without symmetry constraint. These assumptions are reasonable, since d^8 ML_4, d^6 ML_5 and d^6 ML_6 complexes are expected to have roughly square, square-pyramidal and octahedral structure, respectively [10].

In our previous paper [9,10] it was shown that the larger basis set II is required for the better energetics of the critical points on the potential energy surface of the oxidative addition reaction of $RhCl(PH_3)_2$. Therefore, we recalculated the energies of several important alternative structures of reactants, transition states and products at the MP2/II level at the MP2/I optimized geometry. For clarity, we use the standard notation to specify the adopted levels of calculation for energy and structure. For instance, MP2/II//MP2/I designates an MP2 energy calculation with the basis set II using the structure optimized at the MP2 level with the basis set I. All calculations were carried out by using GAUSSIAN 90 and 92 programs [21].

3. Results and discussion

3.1. Reactant $RhCl(CO)(PH_3)_2$

The coordinatively unsaturated 14e complex $Rh(PH_3)_2Cl$, shown as structure I in Fig. 1 and studied in detail in our previous paper [10], has a triplet $^3A_1$ ground state. Its lowest closed shell singlet $^1A_1$ state lies 2–8 kcal mol^{-1} higher than the ground state. One expects that the addition of a CO ligand will stabilize the singlet state much more than the triplet, and the ground state will be a closed shell singlet for the 16e $RhCl(CO)(PH_3)_2$ complex. In general, the CO ligand may attach with the C end to the central Rh atom of $Rh(PH_3)_2Cl$ in three different manners: (a) directly to the empty site in the ClRhPP plane leading to the *trans*-$RhCl(CO)(PH_3)_2$ complex (MP2/I optimized structure II in Fig. 1), (b) within the ClRhPP plane but opening up one of the PRhCl angles leading to the *cis*-$RhCl(CO)(PH_3)_2$ complex (structure III in Fig. 1), and (c) from the direction perpendicular to the ClRhPP plane. Furthermore, the CO molecule can also bind to the central Rh atom with its O atom, leading to isocarbonyl isomers.

The MP2/I optimization under C_1 symmetry for the case (c) converged to structure II, *trans*-$RhCl(CO)(PH_3)_2$ complex, and the perpendicular structure does not exist. As seen in Fig. 1, the *trans*-$RhCl(CO)(PH_3)_2$ complex is about 13 kcal mol^{-1} more stable than the *cis* complex. The former is also calculated to be stable by 73 kcal mol^{-1} relative to the isolated reactants at the MP2/II//MP2/I level, but the absolute value is not certain because of basis set

superposition error and insufficient correlation treatment. The isocarbonyl–*trans*-$RhCl(OC)(PH_3)_2$ isomer (structure IV in Fig. 1) lies about 60 kcal mol^{-1} higher than carbonyl–*trans*-$RhCl(CO)(PH_3)_2$, and is separated from the latter by a small barrier of about 6 kcal mol^{-1} relative to the isocarbonyl isomer at the MP2//II// MP2/I level and may exist only at low temperatures. At higher temperatures it will easily rearrange into the carbonyl–*trans*-$RhCl(CO)(PH_3)_2$ isomer and will not make major contributions to the reaction of $RhCl(CO)(PH_3)_2$ with small molecules. The transition state, MP2/I optimized structure V in Fig. 1, for carbonyl–isocarbonyl isomerization converged to a C_s structure and is a late one, with its structure more resembling structure IV, the isocarbonyl isomer, than structure II, the carbonyl isomer. This is consistent with the large calculated endothermicity of the carbonyl-to-isocarbonyl isomerization. The possible isocarbonyl–carbonyl isomerization for the *cis*-$RhCl(OC)(PH_3)_2$ complex was not studied, as it is also expected to be energetically unfavorable.

As seen in Fig. 1, the CO ligand has a strong trans influence upon addition to $Rh(PH_3)_2Cl$; the Rh–*tL* bond, where *tL* is a ligand positioned trans to CO, is elongated by about 0.06 and 0.12 Å for *tL* = Cl and PH_3, respectively. Meanwhile, the Rh–*cL* bonds, where *cL* is a ligand cis to CO, are stretched only up to 0.02–0.04 Å relative to those in "free" $RhCl(PH_3)_2$ complex. The C–O bonds in carbonyl–$RhCl(CO)(PH_3)_2$ complexes are about 0.03–0.02 Å more stretched than in free CO molecule, while in the isocarbonyl–*trans*-$RhCl(CO)(PH_3)_2$ the C–O distance is nearly unstretched. One should note that the Rh–CO bond in the carbonyl–*trans*-$RhCl(CO)(PH_3)_2$ is about 0.23 Å shorter than Rh–OC distance in the isocarbonyl–*trans*-$RhCl(CO)(PH_3)_2$ isomer, which is consistent with the relative stability of carbonyl and isocarbonyl isomers mentioned above.

3.2. The mechanism of reaction of $RhCl(CO)(PH_3)_2$ with CH_4 and H_2

As was shown above, the *trans*-$RhCl(CO)(PH_3)_2$ and *cis*-$RhCl(CO)(PH_3)_2$ structures are not very differ-

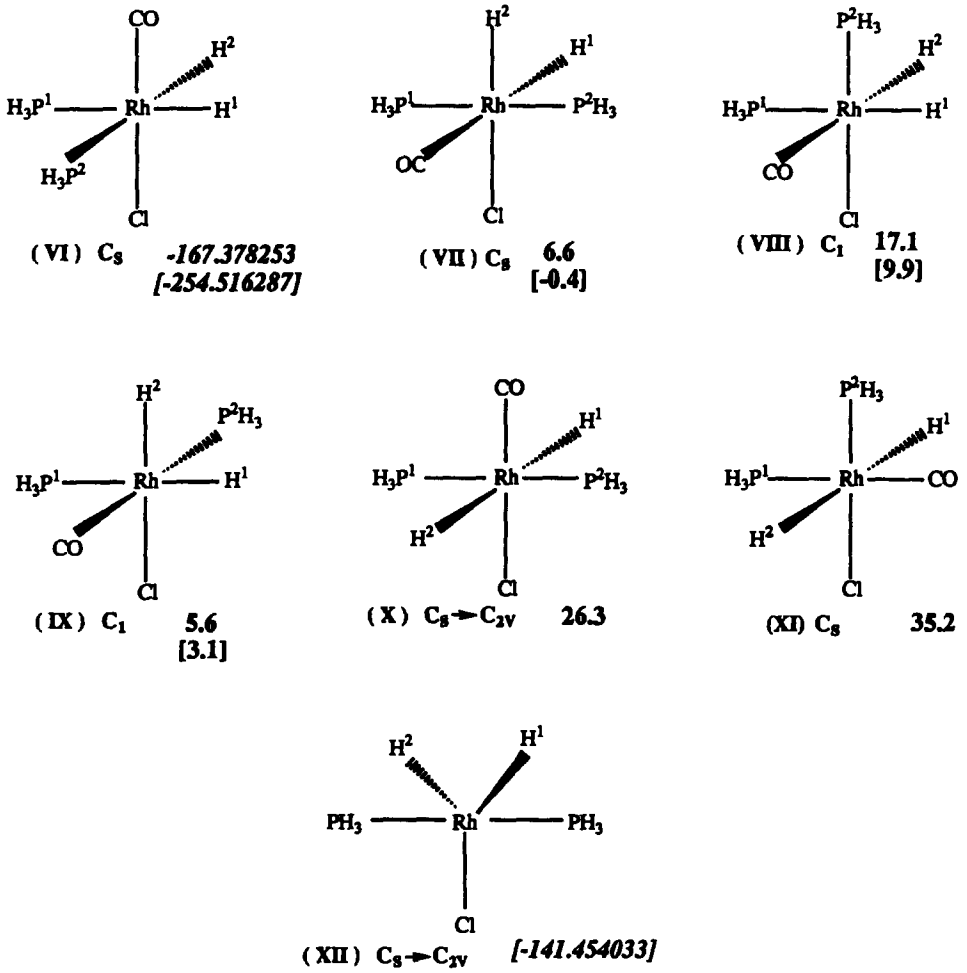

Fig. 2. Structures and energies (total energies in hartrees in italics for reference structures, and relative energies in kcal mol^{-1} for others) of the alternative structures of the $(H)_2RhCl(CO)(PH_3)_2$ complex, as well as $(H)_2RhCl(PH_3)_2$, calculated at the MP2/I//MP2/I and MP2/II// MP2/I (in brackets) level. The optimized geometrical parameters at the MP2/I level are shown in the Table 1. For symmetry notation, see Fig. 1.

Table 1
Optimized geometrical parameters of the alternative structures of $(H)_2RhCl(CO)(PH_3)_2$ and correponding transition states as well as $(H)_2RhCl(PH_3)_2$ at the MP2/I level: distances are in Å, and angles in degrees

Parameter	VI	VII	VIII	IX	X	XI	XII	XIII	XIV	XV	XVI
$Rh-P^1$	2.578	2.356	2.532	2.537	2.352	2.417	2.356	2.513	2.346	2.524	2.440
$Rh-P^2$	2.578	2.356	2.344	2.435	2.352	2.338	2.356	2.513	2.346	2.359	2.485
$Rh-H^1$	1.526	1.573	1.527	1.535	1.665	1.667	1.513	1.658	1.727	1.676	1.865
$Rh-H^2$	1.526	1.537	1.560	1.539	1.665	1.667	1.513	1.658	1.650	1.654	1.859
Rh–C	1.792	1.957	1.961	1.818	1.787	1.820	–	1.766	1.957	1.900	1.769
Rh–Cl	2.446	2.522	2.418	2.520	2.464	2.422	2.462	2.457	2.522	2.396	2.500
P^1-H	1.429	1.423	1.429	1.429	1.421	1.424	1.425	1.428	1.423	1.430	1.430
P^2-H	1.429	1.423	1.426	1.424	1.421	1.425	1.425	1.428	1.423	1.427	1.425
C–O	1.204	1.196	1.195	1.196	1.204	1.196	–	1.210	1.196	1.210	1.206
ClRhC	170.1	94.3	92.2	97.2	180.0	88.1	–	178.4	170.1	97.7	90.2
$ClRhP^1$	89.5	89.9	87.4	88.3	84.0	82.7	91.8	85.2	86.1	85.4	118.2
$ClRhP^2$	89.5	89.9	165.0	85.4	84.0	177.8	91.8	85.2	86.1	174.3	81.3
$ClRhH^1$	87.9	91.5	93.6	94.1	87.9	90.0	145.7	88.0	96.7	86.9	103.8
$ClRhH^2$	87.9	169.3	83.1	173.1	87.9	90.0	145.7	88.0	132.4	86.9	129.3
$CRhP^1$	96.8	90.0	97.1	96.8	95.9	170.8	–	95.6	92.8	102.7	90.7
$CRhP^2$	96.8	90.0	99.6	168.0	95.9	94.1	–	95.6	92.8	84.7	171.5
$CRhH^1$	92.1	174.2	93.6	85.4	92.1	90.0	–	90.4	93.2	123.9	92.8
$CRhH^2$	92.1	96.4	171.4	88.4	92.1	90.0	–	90.4	57.4	161.4	94.1
P^1RhP^2	87.9	176.2	100.0	95.0	168.1	95.1	176.5	102.4	171.9	99.1	93.3
P^1RhH^1	179.5	90.0	166.8	176.6	89.8	90.0	88.2	110.2	89.2	133.4	138.0
P^1RhH^2	92.0	90.1	89.8	88.4	89.8	90.0	88.2	146.0	91.7	95.6	112.5
P^2RhH^1	92.0	90.0	85.8	82.8	89.8	90.0	88.2	146.0	89.2	87.4	89.3
P^2RhH^2	179.5	90.1	84.0	95.1	89.8	90.0	88.2	110.2	91.7	89.2	91.3
H^1RhH^2	88.0	77.8	78.9	82.2	175.8	180.0	68.7	36.2	35.8	38.0	25.6
HP^1Rh	118.6	117.1	118.9	118.6	116.4	117.5	117.6	118.6	117.1	119.0	119.1
HP^2Rh	118.6	117.1	118.1	117.5	116.4	117.5	117.6	118.6	117.1	118.0	117.7
OCRh	177.1	176.3	189.7	179.8	180.0	180.0	–	179.2	177.1	151.8	179.6

ent in energy, and we will study the reactivity of both of them with H_2 and CH_4 molecules.

3.2.1. Reaction of H_2 with $RhCl(CO)(PH_3)_2$

One might expect that the reaction (2) proceeds via a pre-reaction van der Waals complex $(H_2) \cdot RhCl(CO)(PH_3)_2$ to the oxidative addition product $(H)_2RhCl(CO)(PH_3)_2$. However, calculations carried out at the MP2/I level show that the dihydrogen complex $(H_2) \cdot RhCl(CO)(PH_3)_2$ does not exist and dissociates into H_2 and $RhCl(CO)(PH_3)_2$ fragments without a barrier. The octahedral bishydride product $(H)_2RhCl(CO)(PH_3)_2$ may exist in different isomeric forms that could be divided into three classes. The first class, considered to be products of reaction of planar *trans*-$RhCl(CO)(PH_3)_2$, can be obtained by adding H_2 to its empty axial position either (a) within the PRhP plane and bending the same PRhP angle (structure VI in Fig. 2) or

Table 2
The average Rh–X bond distances (in Å) as functions of trans ligands in the alternative structures of $(H)_2RhCl(CO)(PH_3)_2$ and $H(CH_3)RhCl(CO)(PH_3)_2$

Bond Rh–X	trans ligand				
	H	CH_3	CO	P	Cl
For $(H)_2RhCl(CO)(PH_3)_2$ at the MP2/I level					
Rh–Cl	2.521	–	2.483	2.420	–
Rh–P	2.549	–	2.426	–	2.341
Rh–CO	1.959	–	–	1.819	1.790
Rh–H	–	–	1.567	1.531	1.538
For $H(CH_3)RhCl(CO)(PH_3)_2$ at the RHF/I level					
Rh–Cl	2.513	2.510	2.446	2.420	–
Rh–P	2.700	2.626	2.441	2.396	2.385
Rh–CO	2.138	2.100	–	1.906	1.871
$Rh-CH_3$	2.160	–	2.022	2.033	2.064
Rh–H	–	1.623	1.516	1.506	1.528

(b) within the ClRhC plane and bending the same angle (structure VII in Fig. 2). The second class, considered to be products of reaction of planar *cis*-RhCl(CO)$(PH_3)_2$, can be obtained by adding H_2 to its empty axial position either (c) within the PRhC plane and bending the same angle (structure VIII in Fig. 2) or (d) within the PRhCl plane and bending the same angle (structure IX in Fig. 2). The third class includes the structures X and XI, and may be formed only by direct addition of H ligands from the two axial directions of the planar RhCl(CO)$(PH_3)_2$.

As seen in Fig. 2, at the MP2/I//MP2/I level, the structures VIII, X and XI, lying about 17, 26 and 35 kcal mol^{-1} higher, respectively, than the reference structure VI, are not likely to contribute significantly in the present chemistry and will not be considered further. Among the structures VI, VII and IX the energetically lowest is the structure VI, with the structures VII and IX lying about 5–7 kcal mol^{-1} higher. However, a larger basis set at the MP2/II//MP2/I level stabilizes the structures VII–IX a few to several kcal mol^{-1} more than VI and makes the structures VI and VII, the results of reaction of *trans*-RhCl(CO)$(PH_3)_2$ with H_2, more stable by 3 kcal mol^{-1} than the structure IX, the result of reaction of *cis*-RhCl(CO)$(PH_3)_2$.

The MP2/I optimized geometrical parameters of the alternative structures VI–XI are shown in Table 1. The Rh–ligand distances are seen to depend primarily on the ligands trans to them. In order to quantify this trans influence on the bond distances in these octahedral complexes, we have calculated the average Rh–ligand bond distances as functions of the trans ligands, as shown in Table 2. One can clearly see overall that all the bond distances trans to H ligand are much longer than those trans to CO, PH_3 and Cl^- ligands. Among CO, PH_3 and Cl^-, the trans influence seems to decrease in the order: $CO > PH_3 \geq Cl^-$.

The transition states corresponding to the above discussed four different paths (a)–(d) of the reaction (2) have been determined and are shown in Fig. 3 and

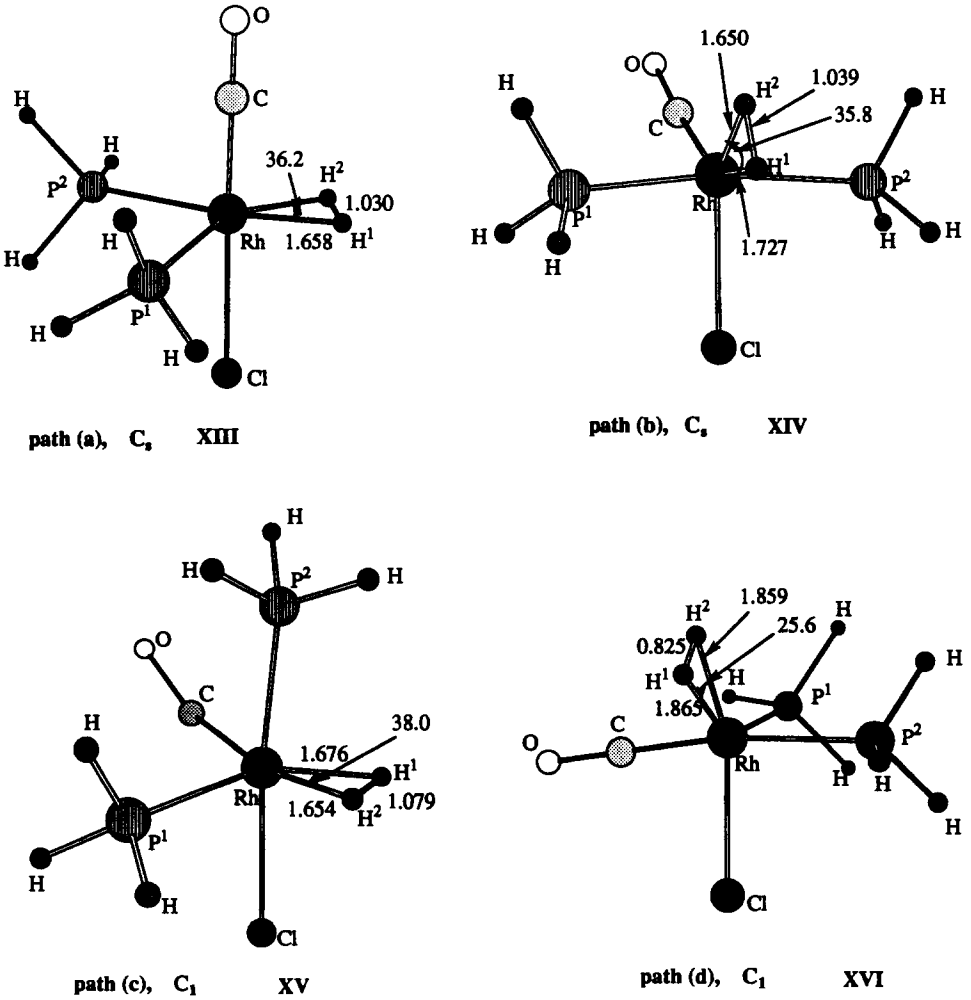

Fig. 3. Transition states for four paths of the reaction RhCl(CO)$(PH_3)_2 + H_2 \rightarrow (H)_2$RhCl(CO)$(PH_3)_2$. Here only some important geometrical parameters (distances in Å and angles in degrees) at the MP2/I level are given. For more parameters see Table 1. Assumed symmetries are also given.

Table 1. Though we have not calculated the exact Hessian at the transition states, the eigenvectors of imaginary frequency of the updated approximate Hessian at the saddle points show that they correspond to lengthening the H–R (R = H and CH_3) bonds being broken. The transition states XIII and XIV, for the paths (a) and (b), e.g., the reaction of H_2 with *trans*-$RhCl(CO)(PH_3)_2$, as well as the transition state XV for path (c) of *cis*-$RhCl(CO)(PH_3)_2$ are late; the H–H distance is elongated significantly and Rh–H bonds are close to those on the products VI and VII, as well as VIII, respectively. However, transition state XVI for path (d) of the reaction of *cis*-$RhCl(CO)(PH_3)_2$ is early; with the H–H bond only slightly elongated and Rh–H bonds substantially longer than in products. This may be related to the largest exothermicity (vide infra) of the path (d) among the four.

As seen in Table 3, where calculated energies of all the present reaction paths for $RhCl(CO)(PH_3)_2 + H_2$ are given, the minimum energy paths for the reaction correspond to the paths (a) and (b), involving the *trans*-$RhCl(CO)(PH_3)_2$ isomer and leading to the products VI and VII, respectively. These two paths are competitive, with barriers of 19.0 and 16.1 kcal mol^{-1}, respectively, and are slightly exothermic, by 1.2 and 1.6 kcal mol^{-1}, respectively, at the MP2/II/MP2/I level. In comparison with these paths of the *trans*-$RhCl(CO)(PH_3)_2$ isomer, the reaction paths (c) and (d) of the *cis*-$RhCl(CO)(PH_3)_2$ isomer are more exothermic, about 4.4 and 11.2 kcal mol^{-1}, respectively, and have similar activation barrier values, 22.1 and 18.3 kcal mol^{-1}, respectively, at the highest MP2/II//MP2/I level. Thus, one may conclude that while the *trans*-$RhCl(CO)(PH_3)_2$ isomer may exist more abundantly than the *cis*-isomer and thus contribute more to the overall reaction, all the four reaction paths studied here have competitive rate constants.

3.2.2. Reaction of CH_4 with $RhCl(CO)(PH_3)_2$

As in the case of reaction (2), one might expect that the reaction (3) proceeds to the oxidative addition product $H(CH_3)RhCl(CO)(PH_3)_2$ via a pre-reaction van der Waals complex $CH_4 \cdot RhCl(CO)(PH_3)_2$. However, calculations carried out at the MP2/I level show that the reactant complex $CH_4 \cdot RhCl(CO)(PH_3)_2$ does not exist and dissociates into CH_4 and $RhCl(CO)(PH_3)_2$ fragments without a barrier. The product complex $H(CH_3)RhCl(CO)(PH_3)_2$ may exist in different isomeric forms. As in the previous section they can be divided into three classes. The first and second of them, structures XVII–XIX and XX–XXIII in Fig. 4, respectively, are the results of reaction of *trans*- and *cis*-$RhCl(CO)(PH_3)_2$ with CH_4, respectively. The third class includes the structures XXIV and XXV, and may be formed only by direct addition of H and CH_3 ligands from the two sides of the planar $RhCl(CO)(PH_3)_2$.

Table 3
The calculated energies of the critical points of the potential energy surfaces of the reaction of $RhCl(CO)(PH_3)_2$ with molecules CH_4 and H_2 [a]

Structure			MP2/I//MP2/I	MP2/II//MP2/I
For the reaction with H_2				
trans-$RhCl(CO)(PH_3)_2 + H_2$			*−167.36746*	*−254.514375*
cis-$RhCl(CO)(PH_3)_2 + H_2$			14.0(0.0) [b]	13.2(0.0)
trans-TS	path (a)	XIII	23.1	19.0
	path (b)	XIV	21.0	16.1
cis-TS	path (c)	XV	41.4(27.3)	35.2(22.1)
	path (d)	XVI	36.0(21.9)	31.4(18.3)
$(H)_2RhCl(CO)(PH_3)_2$		VI	−6.8	−1.2
		VII	−0.2	−1.6
		VIII	10.3(−3.8)	8.7(−4.4)
		IX	−1.2(−15.3)	1.9(−11.2)
For the reaction with CH_4				
trans-$RhCl(CO)(PH_3)_2 + CH_4$			*−206.51980*	*−293.71392*
cis-$RhCl(CO)(PH_3)_2 + CH_4$			14.0(0.0) [b]	13.2(0.0)
Trans-TS		XXVI	31.9	27.3
cis-TS		XXVII	44.6(30.5)	44.4(31.4)
$H(CH_3)RhCl(CO)(PH_3)_2$		XVII	15.5	19.8
$H(CH_3)RhCl(CO)(PH_3)_2$		XXII	16.7(3.5)	21.5(9.3)
BE of the reaction of $HRRhCl(CO)(PH_3)_2 \rightarrow HRRhCl(PH3)2 + CO$				
no H or R [c]			82.5	73.4
R=CH_3			33.2	19.6
R=H				17.0

[a] Total energies (in italics, in hartrees) are given only for reference structures, and relative energies (in kcal mol^{-1}) for other critical points, relative to the reference structures.
[b] In parentheses are energies (in kcal mol^{-1}) relative to *cis*-$RhCl(CO)(PH_3)_2$ + HR, where R=CH_3 and H, respectively.
[c] Energy of the reaction *trans*-$RhCl(CO)(PH_3)_2$ (II) → $RhCl(PH_3)_2 + CO$.

As seen in Fig. 4, at the lowest RHF/I//RHF/I level structures XXII and XXIII are energetically the most favorable, with structures XVII–XIX lying about 4 kcal mol^{-1} higher. Structures XX and XXI and structures XXIV and XXV, lying about 12–13 and 18–22 kcal mol^{-1} higher, respectively, are not likely to contribute significantly in the present chemistry and will not be considered further. At the highest level of theory, MP2/II//MP2/I, used in this paper, structures XVII–XIX, the results of reaction of *trans*-$RhCl(CO)(PH_3)_2$ with CH_4, are stabilized several kcal mol^{-1} more than XXII and become more stable by 2–3 kcal mol^{-1} than the latter, a result of reaction of *cis*-$RhCl(CO)(PH_3)_2$.

The optimized geometrical parameters of the alternative product structures XVII–XXV are shown in Table 4. By using the same approach as in the previous section we have calculated the average Rh–ligand bond distances in these octahedral complexes, in order to quantify the trans influences on the bond distances as functions of the trans ligands, as shown in Table 2 at the RHF level, which is the only level at which all the structures were treated. One can clearly see overall that all the bond distances trans to H and CH_3 ligands are much (by 0.05 Å for the Rh–Cl bond to 0.25 Å for the Rh–P bond) longer than those trans to CO, PH_3 and Cl^- ligands. Between H and CH_3, H seems to have a stronger trans influence than CH_3. CO and PH_3 seem to have very similar trans influences, with CO slightly stronger than PH_3, as in the structures VI–XI. Cl^- ligand, though qualitatively it seems to have a trans influence similar to CO and PH_3, shows a peculiar bond dependence. For Rh–PH_3 and Rh–CO bonds, the trans influence of Cl^- is weaker than those of CO and PH_3, respectively, whereas for Rh–H and Rh–CH_3 bonds, the trans influence of Cl^- is definitely stronger than those of CO and PH_3. One should note that although the inclusion of correlation effects at the MP2/I level of theory decreases all the Rh–ligand bond distances by about 0.05–0.1 Å and changes other bond distances and

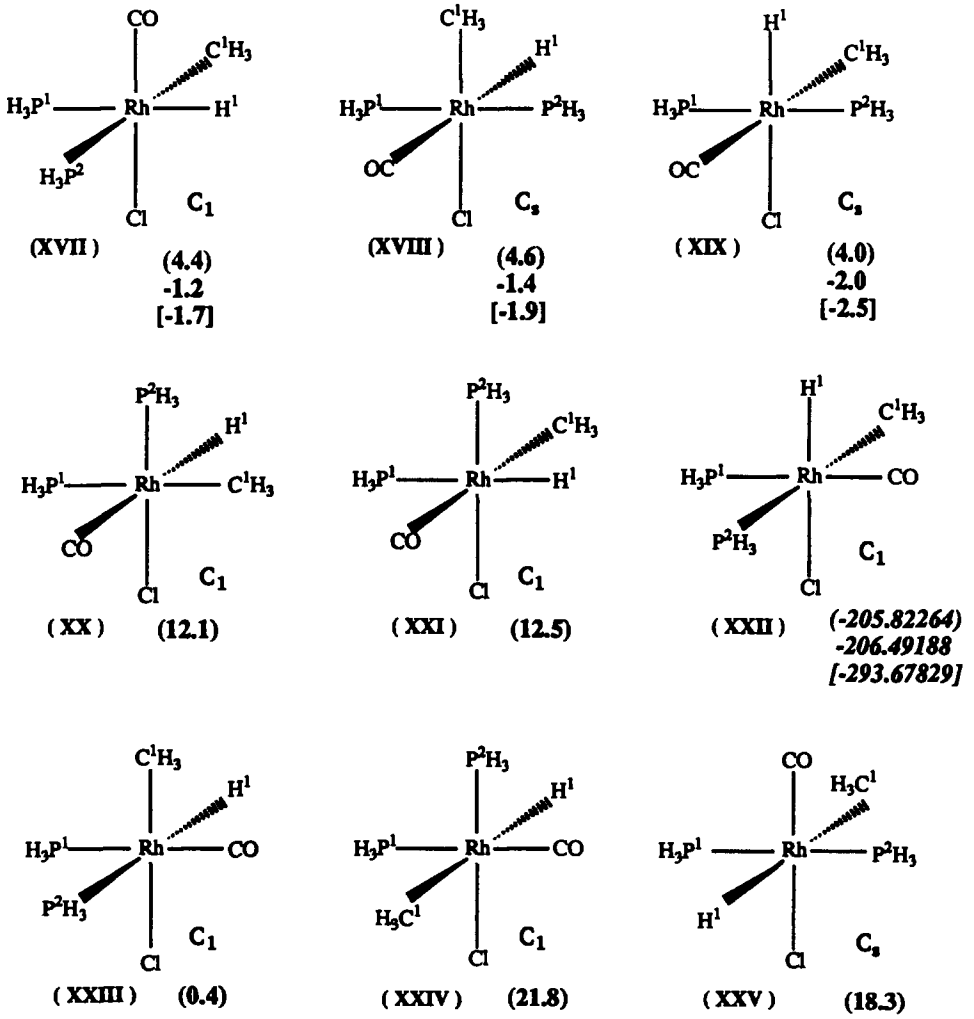

Fig. 4. Structures and energies (total energies in hartrees in italics for reference structure, and relative energies in kcal mol^{-1} for others) of the alternative structures of the $H(CH_3)RhCl(CO)(PH_3)_2$ complex calculated at the RHF/I//RHF/I(in parentheses), MP2/I//MP2/I and MP2/II//MP2/I (in brackets) level. The geometrical parameters are shown in Table 4.

angles slightly (by about 0.01–0.03 Å and 1–3°, respectively), it does not change the above-mentioned conclusion.

For the reaction of CH_4 with $RhCl(CO)(PH_3)_2$ there should exist seven possible paths, three involving *trans*-$RhCl(CO)(PH_3)_2$ to give products XVII to XIX, respectively, and four from *cis*-$RhCl(CO)(PH_3)_2$ to give products XX to XXIII, respectively. In the previous section, we found that within a given class the energies of transition states were similar. Therefore, here we have calculated only one transition state, XXVI, for *trans*-$RhCl(CO)(PH_3)$ to give product XVII and one, XXVII, for *cis*-$RhCl(CO)(PH_3)_2$ to give XXII, as shown in Fig. 5 and Table 4. Both TS XXVI and XXVII are rather tight, with the $Rh-H^1$ bond formation nearly completed, with the $Rh-C^1$ bond about 20% longer than in the product and with the breaking C^1-H^1 bond only about 25–30% longer than free CH_4.

The energetics obtained at the highest level of theory MP2/II//MP2/I, given in Table 3, shows that the reactions (3) of *trans*- and *cis*-$RhCl(CO)(PH_3)_2$ are endothermic by 19.8 and 9.3 kcal mol^{-1} and have barriers of 27.3 and 31.4 kcal mol^{-1}, respectively.

3.2.3. Comparison of the reaction of $RhCl(CO)(PH_3)_2$ with molecules H_2 and CH_4

Here we would like to compare the calculated potential energy surfaces and energies of the reactions (2) and (3) for the more stable *trans*-$RhCl(CO)(PH_3)_2$ isomer of the reactants. As illustrated in Fig. 6, the shapes of potential energy profiles of the reactions (2) and (3) are similar. Both reactions occur with a significant barrier, 16 and 27 kcal mol^{-1}, respectively, and lead to the products without any intermediates. The present results are consistent with previous results showing that, in spite of the similarity between the H–H bond strength of H_2 and the C–H bond strength of CH_4, the H–H bond of the hydrogen molecule is activated more easily than the C–H bond of methane by transition metal complexes [13,22]. The reason for the difference between H–H and C–H activation has been explained [13,22] in terms of the directionality of the bond involving an alkyl group compared to the bond involving hydrogen atoms, as well as in terms of the stronger Rh–H bond compare to the $Rh-CH_3$ bond. Owing to the spherical nature of the H orbital, the Rh–H bond can start to form at the same time as the H–H bond

Table 4
Optimized geometrical parameters of the alternative structures of $H(CH_3)RhCl(CO)(PH_3)_2$, transition states as well as $H(CH_3)RhCl(PH_3)_2$ at the RHF/I and MP2/I (in parentheses) levels: distances are in Å, and angles in degrees

Parameter	XVII	XVIII	XIX	XX	XXI	XXII	XXIII	XXIV	XXV	XXVI	XXVII	XXVIII
$Rh-P^1$	2.689(2.605)	2.404(2.385)	2.407(2.388)	2.616	2.739	2.455(2.459)	2.451	2.417	2.377	(2.578)	(2.473)	(2.365)
$Rh-P^2$	2.628(2.568)	2.404(2.385)	2.407(2.388)	2.384	2.390	2.633(2.557)	2.66	2.380	2.377	(2.458)	(2.451)	(2.365)
$Rh-H^1$	1.507(1.522)	1.514(1.521)	1.524(1.528)	1.518	1.499	1.531(1.541)	1.512	1.623	1.622	(1.573)	(1.585)	(1.504)
Rh–C	1.870(1.779)	2.147(1.961)	2.102(1.914)	2.129	2.098	1.905(1.799)	1.901	1.912	1.872	(1.748)	(1.764)	–
$Rh-C^1$	2.035(2.074)	2.061(2.080)	2.011(2.021)	2.031	2.033	2.033(2.068)	2.067	2.157	2.162	(2.382)	(2.463)	(2.041)
Rh–Cl	2.446(2.455)	2.506(2.514)	2.511(2.519)	2.422	2.424	2.515(2.523)	2.513	2.413	2.445	(2.446)	(2.539)	(2.484)
C^1-H	1.083(1.100)	1.088(1.102)	1.084(1.102)	1.085	1.086	1.084(1.101)	1.083	1.089	1.088	(1.104)	(1.104)	(1.106)
P^1-H	1.413(1.430)	1.407(1.426)	1.408(1.426)	1.411	1.411	1.408(1.426)	1.409	1.408	1.406	(1.430)	(1.426)	(1.426)
P^2-H	1.412(1.430)	1.407(1.426)	1.408(1.426)	1.411	1.410	1.412(1.423)	1.410	1.408	1.406	(1.430)	(1.429)	(1.426)
C–O	1.137(1.207)	1.132(1.219)	1.131(1.217)	1.133	1.133	1.133(1.198)	1.132	1.134	1.137	(1.215)	(1.205)	–
ClRhC	176.5(174.5)	86.4(87.0)	86.1(87.2)	85.8	84.0	93.3(94.8)	90.8	85.1	180.0	(177.4)	(90.3)	–
$ClRhP^1$	83.6(84.0)	89.7(90.1)	91.8(90.1)	86.1	85.5	89.9(89.4)	87.2	85.8	85.7	(90.5)	(86.5)	(90.3)
$ClRhP^2$	87.3(88.0)	89.7(90.1)	91.8(90.1)	173.5	178.5	88.4(88.9)	87.6	179.5	85.7	(89.0)	(96.9)	(90.3)
$ClRhH^1$	93.3(90.7)	93.7(92.7)	179.3(179.7)	89.5	92.5	179.9(176.4)	94.0	91.2	90.8	(90.1)	(149.5)	(140.2)
$ClRhC^1$	88.6(84.9)	177.6(177.7)	94.4(94.7)	89.8	90.1	93.6(90.2)	177.6	85.1	89.1	(90.7)	(119.3)	(145.2)
$CRhP^1$	96.2(96.2)	91.1(90.7)	90.0(90.0)	93.5	88.6	176.8(175.9)	178.0	170.9	94.3	(92.1)	(175.2)	–
$CRhP^2$	96.5(97.4)	91.1(90.7)	90.0(90.0)	100.7	97.5	90.1(90.1)	90.0	94.4	94.3	(90.9)	(90.9)	–
$CRhC^1$	88.0(89.6)	91.2(90.7)	179.6(179.8)	93.6	174.1	89.8(90.0)	89.2	90.6	90.9	(87.9)	(89.1)	–
$CRhH^1$	86.6(89.1)	180.1(179.9)	93.1(92.5)	175.3	94.8	86.7(85.3)	90.0	90.2	89.2	(87.5)	(89.3)	–
P^1RhP^2	87.6(87.2)	182.1(181.4)	176.4(179.3)	93.9	94.5	90.0(90.0)	89.9	94.7	179.9	(104.4)	(93.0)	(178.1)
P^1RhC^1	91.9(92.0)	90.3(89.9)	89.6(89.8)	171.3	88.6	90.0(90.0)	92.8	89.5	90.3	(111.7)	(89.4)	(90.3)
P^1RhH^1	176.8(174.7)	88.9(89.3)	88.2(89.9)	86.1	175.9	90.1(90.6)	90.2	90.0	89.7	(146.4)	(91.8)	(89.0)
P^2RhC^1	175.8(172.9)	90.3(89.9)	90.0(90.0)	90.2	88.4	178.0(179.1)	94.8	88.9	89.5	(143.9)	(143.8)	(89.1)
P^2RhH^1	92.3(92.6)	88.9(89.3)	88.2(89.9)	84.0	87.3	91.4(94.7)	178.4	88.8	90.4	(109.2)	(113.6)	(89.0)
C^1RhH^1	88.0(87.5)	88.6(89.6)	86.4(85.6)	86.4	85.4	86.6(86.2)	83.6	177.6	179.9	(34.8)	(30.2)	–
HP^1Rh	118.3(118.8)	117.1(118.4)	117.2(118.5)	117.9	118.0	117.9(117.4)	117.5	117.4	116.5	(118.9)	(118.0)	(117.6)
HP^2Rh	118.0(118.7)	117.1(118.4)	117.2(118.5)	117.6	117.8	118.0(118.7)	118.0	117.1	116.5	(118.0)	(118.8)	(117.6)
HC^1Rh	110.2(107.8)	111.8(109.3)	111.0(109.1)	110.6	110.9	110.4(108.1)	110.5	111.1	111.3	(109.6)	(110.0)	(109.8)
OCRh	178.6(178.6)	179.7(179.3)	179.8(179.6)	177.8	177.9	179.1(179.2)	179.3	178.3	179.9	(180.7)	(180.5)	–

weakens, whereas the directionality of the CH_3 unpaired orbital forces the C–H bond to break before the new Rh–CH_3 bond forms. Thus there is a smaller barrier for breaking of an H–H bond compared to a C–H bond.

Reaction (3) is endothermic by 19.8 kcal mol^{-1}, while reaction (2) is only 1.6 kcal mol^{-1} exothermic, as seen in Table 3. From the calculated endothermicity of these reactions and H–H and C–H bond energies in the hydrogen and methane molecules, one can calculate the Rh–R (R = H and CH_3) bond strengths using the same technique as in our previous papers [12,13]. Formally, the energy of reaction, ΔE, with a positive (negative) value representing an endothermicity (exothermicity), can be represented using bond energies by

$$\Delta E = D_e(\text{H–R}) - D_e(\text{Rh–R}) - D_e(\text{Rh–H}),$$
$$\text{R} = \text{H and } CH_3 \qquad (6)$$

where Rh stands for the $RhCl(CO)(PH_3)_2$ fragment. At first we note that at the present MP2/II//MP2/I level of theory, the H–R bond energy is calculated to be 99.0 and 108.0 kcal mol^{-1} for the H–H and H–CH_3 bonds, respectively, vs. experimental values of 104.2 and 104.8 kcal mol^{-1}, respectively [20]. Taking the difference of Eq. (6) between two reactions, one obtains

$$\Delta E^{H2} - \Delta E^{CH4} = D_e(\text{H–H}) - D_e(\text{H–CH}_3) - [D_e(\text{Rh–H}) - D_e(\text{Rh–CH}_3)] \qquad (7)$$

Thus, the H–R bond energies and the calculated energies of reaction can be used to estimate the Rh–H and Rh–CH_3 bond energies. From the calculated endothermicity for reaction (2) in Table 3 and the H–R bond energies, Eq. (6) gives the Rh–H bond energy D_e(Rh–H) as 50.3 (52.9) kcal mol^{-1}, obtained by using the calculated and the experimental (in parentheses) H–R bond energies, respectively. From the reaction of H–CH_3 substrates, the application of Eq. (7) gives the Rh–CH_3 bond energy,

$$D_e(\text{Rh–CH}_3) = D_e(\text{Rh–H}) + [D_e(\text{H–CH}_3) - D_e(\text{H–H})] + [\Delta E^{H2} - \Delta E^{CH4}]$$
$$= 50.3\ (52.9) + 9.0\ (0.6) - 21.4$$
$$= 37.9\ (32.1)\ \text{kcal mol}^{-1}$$

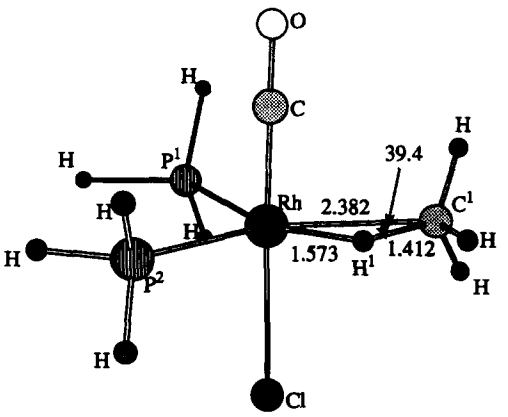

XXVI

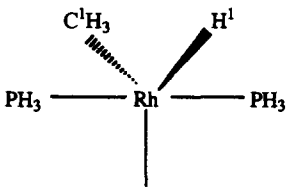

XXVIII

-93.406391
[-180.615331]

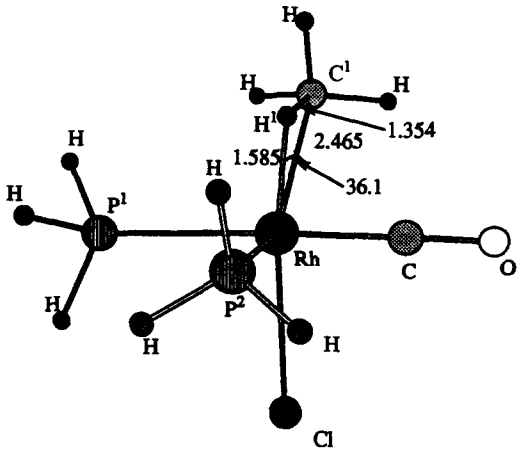

XXVII

Fig. 5. The transition states for the reactions *trans*-$RhCl(CO)(PH_3)_2 + CH_4 \rightarrow H(CH_3)RhCl(CO)(PH_3)_2$ (XXVI) and *cis*-$RhCl(CO)(PH_3)_2 + CH_4 \rightarrow H(CH_3)RhCl(CO)(PH_3)_2$ (XXVII), as well as the structure of the complex $H(CH_3)RhCl(PH_3)_2$. Here only some important geometrical parameters (distances in Å and angles in degrees) at theMP2/I level are given. See Table 4 for more parameters.

The Rh–C bond is 12.4 (20.8) kcal mol^{-1} weaker than the Rh–H bond.

As shown in Table 3, the CO binding energy in four-coordinate OC–$RhCl(PH_3)_2$ is calculated to be 73 kcal mol^{-1} at the MP2/II//MP2/I level. The addition of the two H or one H and one CH_3 ligands to $RhCl(CO)PH_3)_2$ dramatically decreases the Rh–CO binding energy to 17 or 20 kcal mol^{-1}, respectively. Thus, one may conclude that the CO molecule can dissociate from the product $H(R)RhCl(CO)(PH_3)_2$ at moderate temperatures. This conclusion is in good agreement with the latest experiment [7].

Since the present calculation of the bonding energies has been carried out at the relatively low MP2 level with a modest basis set, absolute values of the Rh–H, Rh–CH_3 and Rh–CO bond energies may contain some errors due to approximate electron correlation treatment, basis functions and basis set superposition error.

3.3. Comparison of reactions of $RhCl(PH_3)_2$ and $RhCl(CO)(PH_3)_2$

Here we would like to compare the PESs and energies of the present reactions of the 16e four-coordinate complex:

$$trans\text{-}RhCl(CO)(PH_3)_2 + H_2 \rightarrow (H)_2RhCl(CO)(PH_3)_2 \quad (2)$$

$$trans\text{-}RhCl(CO)(PH_3)_2 + CH_4 \rightarrow H(CH_3)RhCl(CO)(PH_3)_2 \quad (3)$$

with the analogous reactions for the 14e three-coordinate complex without a CO ligand.

$$RhCl(PH_3)_2 + H_2 \rightarrow (H)_2RhCl(PH_3)_2 \quad (4)$$

$$RhCl(PH_3)_2 + CH_4 \rightarrow H(CH_3)RhCl(PH_3)_2 \quad (5)$$

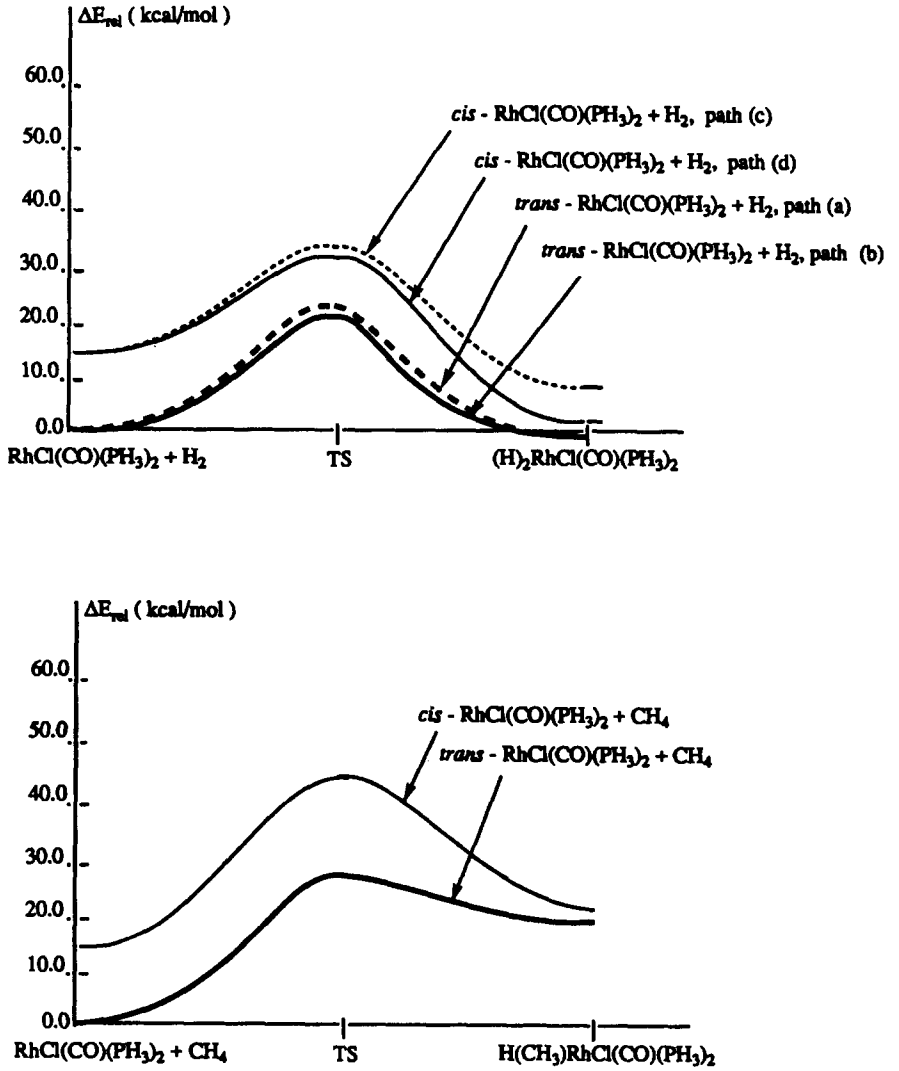

Fig. 6. Potential energy profiles of reaction $RhCl(CO)(PH_3)_2 + HR \rightarrow H(R)RhCl(CO))(PH_3)_2$ calculated at the MP2/II//MP2/I level, where R = H and CH_3.

As mentioned above, the reactions (4) and (5) have been studied in detail by Koga and Morokuma [9,10]. It has been found that in the first step the reactions (4) and (5) yield molecular complexes, $(CH_4)\cdot RhCl(PH_3)_2$ and $(H_2)\cdot RhCl(PH_3)_2$, which are stable relative to the isolated reactants by 17 and 20 kcal mol^{-1}, respectively. Then the C–H and H–H bond activation takes place with 3 and 0.6 kcal mol^{-1} activation barriers relative to CH_4 and H_2 complexes, respectively. The entire reactions are exothermic by 24 and 26 kcal mol^{-1}, for CH_4 and H_2 reactions, respectively. Again the absolute values should not be taken too seriously.

Thus, comparison of the reactions (4) and (5) with (2) and (3), respectively, shows that addition of a CO ligand to the 14e coordinatively unsaturated $RhCl(PH_3)_2$ complex dramatically changes its reactivity. First, are no molecular complexes on the PES of the 16e saturated complex $RhCl(CO)(PH_3)_2$; the complexes $(H_2)\cdot RhCl(CO)(PH_3)_2$ and $(CH_4)\cdot RhCl(CO)(PH_3)_2$ are not kinetically and energetically stable relative to the reactants. Second, there appear significant H–H and C–H bond activation barriers. Third, the exothermicity of the entire reactions decreases, and as a result the reaction (3) becomes endothermic by 19.8 kcal mol^{-1} while the reaction (2) still remains exothermic but only by 1.6 kcal mol^{-1}. All the above-mentioned differences in the reactivity between the unsaturated 14e complex $RhCl(PH_3)_2$ and the saturated 16e $RhCl(CO)(PH_3)_2$ complex may be explained in terms of saturation of the coordination sphere of the transition metal atoms. The saturation of the $RhCl(PH_3)_2$ complex with a strong CO ligand (with a complexation energy calculated to be 73.4 kcal mol^{-1}) makes its interaction with weak H_2 and CH_4 ligands unfavorable, and makes Rh–H and $Rh-CH_3$ (where Rh stands for the $RhCl(CO)(PH_3)_2$ fragment) bonds weaker. Indeed, as was reported by Koga and Morokuma [12], the $Cl(PH_3)_2Rh-H$ and $Cl(PH_3)_2Rh-CH_3$ bond strengths are 65.1 and 54.6 kcal mol^{-1}, which are about 15 and 17 kcal mol^{-1}, respectively, larger than the 50.3 and 37.9 kcal mol^{-1} for $Cl(CO)(PH_3)_2Rh-H$ and $Cl(CO)(PH_3)_2Rh-CH_3$ reported in this paper.

Thus, the unsaturated character of $RhCl(PH_3)_2$ makes it reactive with alkanes and hydrogen. Coordination of an additional ligand to the central Rh atom saturates this complex and makes it unreactive with alkanes and hydrogen at moderate temperatures. Similar conclusions have been obtained in experiments: *trans*-$RhCl(PPh_3)_2$ is more reactive with alkanes than its carbonyled *trans*-$RhCl(CO)(PPh_3)_2$ derivative [7] and $RhCl(PMe_3)_2$ generated by flash photolysis of *trans*-$RhCl(CO)(PMe)_2$ derivative reacts very rapidly with hydrocarbons [3].

4. Conclusions

We can summarize our conclusions as follows.

1. The reaction $RhCl(PH_3)_2 + CO$ is exothermic by 73 kcal mol^{-1}, and leads to formation the complex $RhCl(CO)(PH_3)_2$, which may exist in *trans*- and *cis*-isomeric forms. The *trans*-$RhCl(CO)(PH_3)_2$ is calculated to be more stable by 13 kcal mol^{-1} than *cis*-$RhCl(CO)(PH_3)_2$. Isocarbonyl *trans*-$RhCl(OC)(PH_3)_2$ lies about 60 kcal mol^{-1} higher than carbonyl *trans*-$RhCl(CO)(PH_3)_2$, is separated from the latter by a small (about 6 kcal mol^{-1} relative to the isocarbonyl complex) barrier, and may exist only at low temperatures. At higher temperatures it will easily rearrange into the corresponding carbonyl isomer, and will not make any major contribution to the mechanism of reaction of the $RhCl(CO)(PH_3)_2$ complex with small molecules.

2. Addition of a CO ligand to $RhCl(PH_3)_2$ dramatically changes the reactivity of this Rh complex with molecular hydrogen and alkanes. Although the reactions of $RhCl(PH_3)_2$ with H_2 and CH_4 molecules occur very fast (with a few kcal mol^{-1} activation barrier) and are exothermic (about 26 and 24 kcal mol^{-1}, respectively), the reactions of $RhCl(CO)(PH_3)_2$:

$$\textit{trans}\text{-}RhCl(CO)(PH_3)_2 + H_2 \rightarrow (H)_2RhCl(CO)(PH_3)_2 \quad (2)$$

and

$$\textit{trans}\text{-}RhCl(CO)(PH_3)_2 + CH_4 \rightarrow H(CH_3)RhCl(CO)(PH_3)_2 \quad (3)$$

are endothermic by 20 and exothermic only by 2 kcal mol^{-1}, and have about 27 and 16 kcal mol^{-1} barriers (relative to reactants), respectively. Thus, they do not take place under moderate conditions. On the PESs of the reactions (2) and (3) there is no intermediate corresponding to the H_2 and CH_4 complexes, respectively. The much reduced reactivity of $RhCl(CO)(PH_3)_2$ as compared with $RhCl(PH_3)_2$ agrees with the recent experiments [3,7].

3. The reaction of H_2 with the higher energy *cis*-$RhCl(CO)(PH_3)_2$ isomer is calculated to be exothermic by 11 kcal mol^{-1}, while the analogous reaction of CH_4 is endothermic by 9 kcal mol^{-1}. Both reactions have significant activation barriers of 18 and 31 kcal mol^{-1}, respectively, relative to the reactants, and will not make major contributions to the mechanism of reaction of $RhCl(CO)(PH_3)_2$ with small molecules.

4. The binding energy $OC-[H(R)RhCl(PH_3)_2]$ is calculated to be 17 and 20 kcal mol^{-1}, respectively, for $R = H$ and CH_3. Thus, one may conclude that the CO

molecule may dissociate from the product H(R)RhCl $(CO)(PH_3)_2$ at moderate temperatures. This conclusion is also in good agreement with the latest experiment [7].

5. The calculated binding energies for Rh–H and $Rh–CH_3$ bonds in the $(H)_2RhCl(OC)(PH_3)_2$ and $H(CH_3)RhCl(CO)(PH_3)_2$ complexes are 50 and 38 kcal mol^{-1}, respectively, e.g., 15 and 17 kcal mol^{-1} smaller than those (65 and 55 kcal mol^{-1}) for uncarbonyled complexes $(H)_2RhCl(PH_3)_2$ and $H(CH_3)RhCl(PH_3)_2$, respectively, reported by Koga and Morokuma [11].

Acknowledgement

The present research is in part supported by a grant (CHE-9409020) from the National Science Foundation.

References

[1] A.E. Shilov, *Activation of Saturated Hydrocarbons*, Reidel, Dordrecht, 1984.
[2] T. Sakakura and M. Tanaka, *Chem. Lett., 249* (1987) 1113.
[3] C.T. Spillet and P.C. Ford, *J. Am. Chem. Soc., 111* (1989) 1932.
[4] J.A. Osborn, F.H. Jardine, J.F. Young and Wilkilson, G. *J. Chem. Soc. A*, (1966) 1711.
[5] (a) F. Charentenay, J.A. Osborn and Wilkilson, G. *J. Chem. Soc. A* (1968) 787. (b) J.A. Maguire, W.T. Boese and A.S. Goldman, *J. Am. Chem. Soc., 111* (1989) 7088. (c) J.A. Maguire and A.S. Goldman, *J. Am. Chem. Soc., 113* (1991) 6706. (d) J.A. Maguire, A. Petrillo and A.S. Goldman, *J. Am. Chem. Soc., 114* (1992) 9492. (e) K.C. Shih and A.S. Goldman, *Organometallics, 12* (1993) 3390.
[6] (a) L. Vaska and J.W. DiLuzio, *J. Am. Chem. Soc., 84* (1962) 679 (b) R. Ugo, A. Pasini, A. Fusi and S. Cenini, *J. Am. Chem. Soc., 94* (1972) 7364 (c) M.J. Burk, M.P. McGrath, R. Wheeler and R.H. Crabtree, *J. Am. Chem. Soc., 110* (1988) 5034 (d) F. Abu-Hasanayn, K. Krogh-Jespersen and A.S. Goldman, *J. Am. Chem. Soc., 115* (1993) 8019. (e) F. Abu-Hasanayn, A.S. Goldman and K. Krogh-Jespersen, *Inorg. Chem., 32* (1993) 495. (f) F. Abu-Hasanayn, A.S. Goldman and K. Krogh-Jespersen, *Inorg. Chem., 33* (1994) 5122. (g) F. Abu-Hasanayn, A.S. Goldman and K. Krogh-Jespersen, *J. Phys. Chem., 97* (1993) 5890. (h) F. Abu-Hasanayn, A.S. Goldman and K. Krogh-Jespersen, *Organometallics, 13* (1994) 5177. (i) A.L. Sargent and M.B. Hall, *Inorg. Chem., 31* (1992) 317. (j) A.L. Sargent, M.B. Hall and M.F. Guest, *J. Am. Chem. Soc., 114* (1992, 517.
[7] S.B. Duckett and R. Eisenberg, *J. Am. Chem. Soc., 115* (1993) 5292.
[8] (a) A. Dedieu and A. Strich, *Inorg. Chem., 10* (1979) 2940. (b) A. Sevin, *Nouv. J. Chim., 5* (1981) 233. (c) J.Y. Saillard and R. Hoffmann, *J. Am. Chem. Soc., 106* (1984) 2006. (d) Y. Jean and A. Lledos, *Nouv. J. Chim., 10* (1986) 635.
[9] C. Daniel, N. Koga, J. Han, X.Y. Fu and Morokuma, K. *J. Am. Chem. Soc., 110* (1988) 3773.
[10] N. Koga and K. Morokuma, *J. Phys. Chem., 94* (1990) 5454.
[11] S. Obara, K. Kitaura and K. Morokuma, *J. Am. Chem. Soc., 106* (1984) 7482.
[12] N. Koga and K. Morokuma, *J. Am. Chem. Soc., 115* (1993) 6883.
[13] D.G. Musaev and K. Morokuma, *J. Am. Chem. Soc., 117* (1995) 799.
[14] (a) D.G. Musaev and K. Morokuma, *Isr. J. Chem., 33* (1993) 307, and references therein (b) D.G. Musaev and K. Morokuma, *J. Chem. Phys., 101* (1994) 10697.
[15] N. Koga and K. Morokuma, *Chem. Rev., 91* (1991) 823.
[16] T.H. Dunning, Jr., *J. Chem. Phys., 53* (19700 2823.
[17] P.J. Hay and W.R. Wadt, *J. Chem. Phys., 82* (1985) 270.
[18] P.J. Hay and W.R. Wadt, *J. Chem. Phys., 82* (1985) 284.
[19] T.H. Dunning, Jr. and P.J. Hay, in H.F. Schaeffer (ed.), *The Methods of Electronic Structure Theory*, Plenum, New York, 1977.
[20] P.J. Hay and W.R. Wadt, *J. Chem. Phys., 82* (1985) 299.
[21] M.J. Frisch, G.W. Trucks, M. Head-Gordon, P.M.W. Gill, M.W. Wong, J.B. Foresman, B.G. Johnson, H.B. Schlegel, M.A. Robb, E.S. Replogle, R. Gomperts, J.L. Andres, K. Raghavachari, J.S. Binkley, C. Gonzales, R.L. Martin, D.J. Fox, D.J. DeFrees, J. Baker, J.J.A. Stewart and J.A. Pople, *GAUSSIAN-92*, Gaussian Inc., Pittsburgh, PA, 1992.
[22] (a) M.R.A. Blomberg, P.E.M. Siegbahn and Svensson, M. *J. Phys. Chem., 95* (1991) 4313 (b) M.R.A. Blomberg, P.E.M. Siegbahn and M. Svensson, *New J. Chem., 15* (1991,) 727.
[23] *CRC Handbook of Chemistry and Physics*, CRC Press, Boca Raton, 72nd edn., 1991–1992.